

Discovery of Aminopyridine-Based Inhibitors of Bacterial Enoyl-ACP Reductase (FabI)

William H. Miller,* Mark A. Seefeld, Kenneth A. Newlander, Irene N. Uzinskas, Walter J. Burgess, Dirk A. Heerding, Catherine C. K. Yuan, Martha S. Head, David J. Payne, Stephen F. Rittenhouse, Terrance D. Moore, Stewart C. Pearson, Valerie Berry, Walter E. DeWolf, Jr., Paul M. Keller, Brian J. Polizzi, Xiayang Qiu, Cheryl A. Janson, and William F. Huffman

GlaxoSmithKline Pharmaceuticals, 1250 South Collegeville Road, P.O. Box 5089, Collegeville, Pennsylvania 19426

Received February 1, 2002

Bacterial enoyl-ACP reductase (FabI) catalyzes the final step in each cycle of bacterial fatty acid biosynthesis and is an attractive target for the development of new antibacterial agents. Our efforts to identify potent, selective FabI inhibitors began with screening of the GlaxoSmithKline proprietary compound collection, which identified several small-molecule inhibitors of *Staphylococcus aureus* FabI. Through a combination of iterative medicinal chemistry and X-ray crystal structure based design, one of these leads was developed into the novel aminopyridine derivative **9**, a low micromolar inhibitor of FabI from *S. aureus* ($IC_{50} = 2.4 \mu\text{M}$) and *Haemophilus influenzae* ($IC_{50} = 4.2 \mu\text{M}$). Compound **9** has good in vitro antibacterial activity against several organisms, including *S. aureus* ($MIC = 0.5 \mu\text{g/mL}$), and is effective in vivo in a *S. aureus* groin abscess infection model in rats. Through FabI overexpressor and macromolecular synthesis studies, the mode of action of **9** has been confirmed to be inhibition of fatty acid biosynthesis via inhibition of FabI. Taken together, these results support FabI as a valid antibacterial target and demonstrate the potential of small-molecule FabI inhibitors for the treatment of bacterial infections.

Introduction

The emergence of antibiotic-resistant pathogens is a serious health problem worldwide.^{1–4} Certain infections that were previously treatable with standard antibiotic therapies can now be caused by multidrug-resistant organisms that are no longer susceptible to conventional treatment. For example, methicillin-resistant *Staphylococcus aureus* (MRSA) and vancomycin-resistant enterococci (VRE) are major concerns in hospital settings, and multidrug-resistant strains of *Streptococcus pneumoniae*, *Streptococcus pyogenes*, *Mycobacterium tuberculosis*, *Neisseria gonorrhoeae*, and *Escherichia coli* plague the community.

One approach to combating antibiotic resistance is to identify new drugs that function through novel mechanisms of action. In this regard, bacterial fatty acid biosynthesis (FAS) is an attractive antibacterial target.⁵ Bacterial FAS is an essential process by which organisms make fatty acids for use in the assembly of important cellular components, including phospholipids, lipoproteins, lipopolysaccharides, mycolic acids, and the cell envelope. Since FAS is organized differently in bacteria and mammals, there is good potential for selective inhibition of the bacterial system. In bacteria, each reaction involved in FAS is catalyzed by a discrete monofunctional enzyme (the fatty acid synthase II, or FAS II, system; see Figure 1), whereas in mammals, all of the enzymatic activities involved in FAS are encoded on one or two polypeptide chains (the FAS I system).

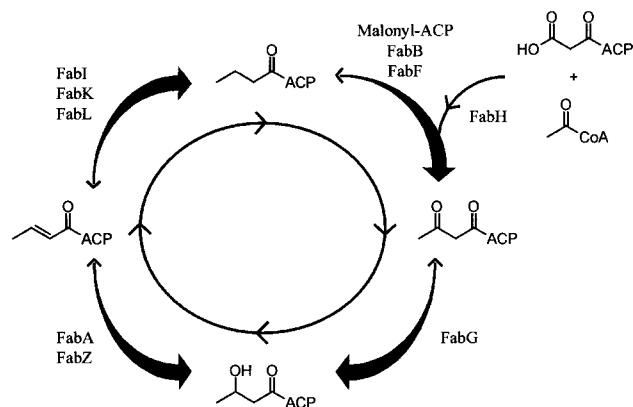
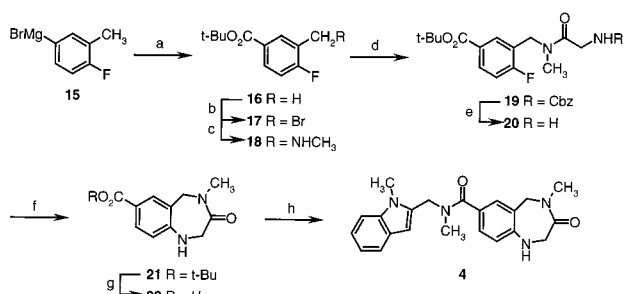


Figure 1. Schematic representation of bacterial fatty acid biosynthesis.

The final step in each cycle of bacterial FAS is catalyzed by an enoyl-ACP reductase, which mediates the 1,4-reduction of an enoyl-ACP to the corresponding acyl-ACP and drives each cycle of FAS to completion.^{5,6} Until recently, FabI was believed to be the unique enoyl-ACP reductase in bacteria.^{5,7} FabI is a monofunctional, NADH- or NADPH-dependent enzyme^{8,9} that has been shown to be the antibacterial target of the diazaborines^{10,11} as well as triclosan,^{12–16} a widely used antibacterial agent that is added to a variety of consumer products including toothpastes, mouthwashes, and hand soap. Although early studies seemed to suggest that FabI might be essential in all bacteria, an alternative triclosan-resistant enoyl-ACP reductase, termed FabK, has recently been identified in several organisms.⁷ FabK, a flavoprotein, is the sole enoyl-ACP reductase in *S. pneumoniae* and occurs together with FabI in key

* To whom correspondence should be addressed. Phone: 610-917-7937. Fax: 610-917-4206. E-mail: william_h_miller@gsk.com.

Scheme 1. Synthesis of 1,4-Benzodiazepine Derivative **4**^a

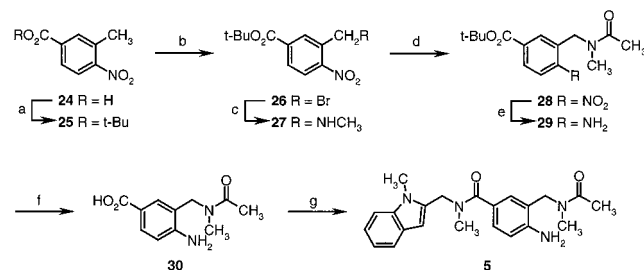
^a Reagents: (a) (Boc)₂O, THF (94%); (b) NBS, CCl₄, reflux, *hν*; (c) CH₃NH₂ (aq), THF, 0 °C to room temp (43% for two steps); (d) *N*-Cbz-Gly, DCC, HOBT·H₂O, 1:1 DMF/CH₂Cl₂ (100%); (e) H₂ (50 psi), 10% Pd/C, MeOH; (f) DMSO, 125 °C (48% for two steps); (g) TFA, CH₂Cl₂, then 4 N HCl in dioxane; (h) 1-methyl-2-(methylaminomethyl)indole (**23**), EDC, HOBT·H₂O, Et₃N, 1:1 DMF/CH₂Cl₂ (92% for two steps).

pathogens such as *Enterococcus faecalis* and *Pseudomonas aeruginosa*. A third enoyl-ACP reductase, termed FabL, occurs together with FabI in *Bacillus subtilis*.¹⁷ Consequently, a pure FabI or FabK inhibitor is expected to be a narrow-spectrum agent that targets a few organisms, or possibly even a single organism, while an inhibitor of both FabI and FabK is expected to have broader-spectrum activity. In certain circumstances, the use of narrow-spectrum agents may offer advantages over broad-spectrum agents.^{2,3} Inhibitors of FabI might also have utility in the treatment of malaria,^{18–21} since triclosan has recently been shown to inhibit the enoyl-ACP reductase of the parasite *Plasmodium falciparum*.

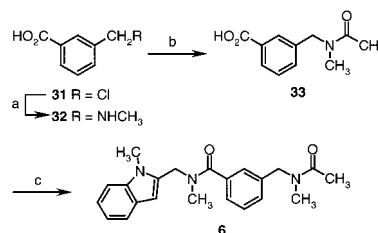
Our approach to the identification of small-molecule FabI inhibitors began with screening of the Glaxo-SmithKline proprietary compound collection to identify novel lead compounds that inhibit *S. aureus* FabI. Optimization of these screening leads involved a combination of iterative medicinal chemistry as well as X-ray crystal structure based design. We previously reported the transformation of two of these leads into potent FabI inhibitors with good antibacterial activity against *S. aureus*.^{22,23} In the present report, we describe our investigation of a third lead, benzodiazepine **1**, which led to the identification of a novel aminopyridine-based FabI inhibitor with good antibacterial activity against *S. aureus*.

Chemistry

The 1,4-benzodiazepine derivatives **2–4** were prepared according to the general literature procedures for the synthesis of related 1,4-benzodiazepines.^{24,25} The synthesis of compound **4** illustrates the method (Scheme 1). Commercially available 4-fluoro-3-methylphenylmagnesium bromide (**15**) reacted with di-*tert*-butyl dicarbonate to give the *tert*-butyl benzoate **16**. Reaction of **16** with NBS gave the benzylic bromide **17**, which, without purification, was converted to benzylic amine **18** by reaction with aqueous methylamine. Acylation of **18** with *N*-(benzyloxycarbonyl)glycine in the presence of DCC and HOBT afforded **19**. Hydrogenolysis of the Cbz protecting group gave **20**, which cyclized in hot DMSO to afford the benzodiazepine **21**. Deprotection of the *tert*-butyl ester under acidic conditions gave the corresponding carboxylic acid (**22**), which was coupled

Scheme 2. Synthesis of Compound **5**^a

^a Reagents: (a) PhSO₂Cl, *tert*-BuOH, pyridine (95%); (b) NBS, benzoyl peroxide, CH₂Cl₂; (c) 40% CH₃NH₂ in H₂O (76% for two steps); (d) Ac₂O, (*i*-Pr)₂NEt, CH₂Cl₂; (e) H₂, 10% Pd/C, MeOH (85% for two steps); (f) TFA, CH₂Cl₂ (quantitative) (g) **23**, EDC, HOBT·H₂O, (*i*-Pr)₂NEt, DMF (89%).

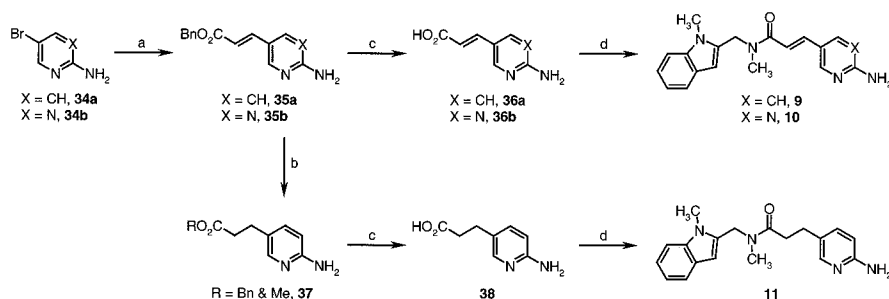
Scheme 3. Synthesis of Compound **6**^a

^a Reagents: (a) 2 M CH₃NH₂ in MeOH; (b) Ac₂O, Et₃N, CHCl₃ (53% for two steps); (c) **23**, EDC, HOBT·H₂O, Et₃N, CH₂Cl₂ (86%).

with 1-methyl-2-(methylaminomethyl)indole (**23**; prepared by reductive amination of commercially available 1-methylindole-2-carboxaldehyde) in the presence of EDC and HOBT to afford the target compound **4**. The related compounds **2** and **3** were prepared by coupling **23** to the corresponding known^{24,25} (*R*)- and (*S*)-benzodiazepine-7-carboxylic acid derivatives.

The benzamide derivatives **5–8** were prepared either by standard methods or as illustrated in Schemes 2 and 3. The synthesis of **5** began with esterification²⁶ of 3-methyl-4-nitrobenzoic acid (**24**) to afford *tert*-butyl ester **25**. Benzylic bromination gave the corresponding crude benzylic bromide **26**,²⁷ which reacted with aqueous methylamine in THF to give the benzylic amine **27**. Acylation with acetic anhydride gave **28**, which on hydrogenation gave **29**. Cleavage of the *tert*-butyl ester under standard acidic conditions, followed by coupling with 1-methyl-2-(methylaminomethyl)indole (**23**), gave compound **5**. The related benzamide derivative **6** was prepared similarly, as illustrated in Scheme 3, and the benzamides **7** and **8** were prepared by coupling **23** with commercially available carboxylic acids.

The aminopyridine derivatives and related analogues were prepared either by standard methods or as described in Scheme 4. Commercially available 2-amino-5-bromopyridine (**34a**) or 2-amino-5-bromopyrimidine (**34b**) was reacted with benzyl acrylate in a Heck-type reaction²⁸ to afford the acrylate esters **35a** and **35b**, respectively. These were saponified to provide acids **36a** and **36b**, which were coupled with **23** to give **9** and **10**, respectively. Alternatively, for the synthesis of **9**, a Heck reaction of **34a** with acrylic acid provided **36a** directly. For the synthesis of **11**, the olefin of **35a** was reduced with magnesium metal in methanol, and the resulting mixture of benzyl and methyl esters **37** was saponified. The resulting carboxylic acid **38** was coupled with **23** to give **11**. The aminonicotinamide derivative **12** and

Scheme 4. Synthesis of Compounds **9–11**^a

^a Reagents: (a) benzyl acrylate, Pd(OAc)₂, P(*o*-tol)₃, (*i*-Pr)₂NEt, propionitrile (39% for **35a**, 79% for **35b**); (b) Mg, MeOH; (c) 1.0 N NaOH, MeOH, then H₃O⁺ (72% for **36a**, 90% for **36b**, 83% for two steps for **38**); (d) **23**, EDC, HOBT·H₂O, Et₃N, DMF (83% for **9**, 89% for **10**, 46% for **11**).

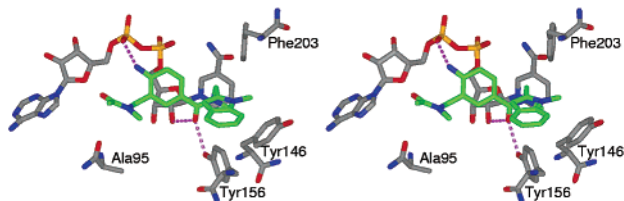


Figure 2. Representation of the X-ray crystal structure of **5** bound to *E. coli* FabI/NAD⁺.

the acrylate derivatives **13** and **14** were prepared by coupling **23** with commercially available carboxylic acids.

Results and Discussion

Screening of the GlaxoSmithKline (GSK) proprietary compound collection identified the 1,4-benzodiazepine derivative **1** (Table 1) as a low micromolar inhibitor of FabI from *S. aureus* and *Haemophilus influenzae* (IC₅₀ = 16.5 and 6.9 μM, respectively). However, **1** does not appreciably inhibit *S. pneumoniae* FabK (IC₅₀ > 30 μM) and has poor antibacterial activity, with MIC = 32 μg/mL against *Moraxella catarrhalis* and MIC > 64 μg/mL against *S. aureus*, *E. coli* AcrAB⁻ (an efflux mutant), *H. influenzae*, *E. faecalis*, and *S. pneumoniae*. Nevertheless, we pursued this lead with the expectation that antibacterial activity might improve as potency against the target improved.

Evaluation of several derivatives structurally related to **1** revealed the importance of the indole, or an appropriate, lipophilic bioisostere thereof, to FabI activity. For example, 1,4-benzodiazepine derivatives wherein the indole group is replaced with phenyl, 2-quinoline, 2-benzoxazole, 2-benzothiazole, or 2-benzimidazole are all much weaker inhibitors of *S. aureus* FabI. However, a 2-naphthalene derivative has activity comparable to that of **1** in the FabI assay (data not shown). Therefore, for the purposes of our initial studies, the indole subunit was maintained as a constant while we focused on the identification of the minimum key pharmacophoric elements within the benzodiazepine subunit.

Since **1** is racemic, we prepared the corresponding (*R*)- and (*S*)-enantiomers and found that the (*R*)-enantiomer **2** is clearly preferred by FabI. However, when the ester side chain is removed altogether, the resulting compound **4** has activity comparable to that of **2** in the FabI assays and now has modest antibacterial activity against *S. aureus* (MIC = 16 μg/mL). These results show that the ester side chain of **2** is not a key pharmacophoric element for inhibition of FabI. None of these benzodi-

azepine derivatives appreciably inhibits *S. pneumoniae* FabK (IC₅₀ > 30 μM).

The importance of the benzodiazepine ring was explored through an investigation into ring-opened variants of **4**. The trisubstituted benzamide derivative **5** maintains FabI inhibitory activity as well as antibacterial activity against *S. aureus*, indicating that the seven-membered ring of **4** is not necessary for activity. Further simplification by removal of the amino group from **5** to give derivative **6** causes a substantial decrease in activity. In contrast, removal of the acetyl amino side chain of **5** to give the *p*-aminobenzamide derivative **7** causes only a modest decrease in activity against *S. aureus* FabI, and antibacterial activity against *S. aureus* is maintained. These results suggest the importance of the para amino group for FabI inhibition and antibacterial activity. In support of this hypothesis, the simple benzamide derivative **8** is much less active in the FabI assay and has no detectable antibacterial activity up to 64 μg/mL. None of these benzamide derivatives appreciably inhibits *S. pneumoniae* FabK (IC₅₀ > 30 μM).

Since the *p*-aminobenzamide functionality present in both **5** and **7** appeared to represent the minimum pharmacophore for both FabI inhibitory activity as well as antibacterial activity, we began an investigation of these new leads. As part of this study, we determined the X-ray cocrystal structure of **5** (*E. coli* FabI IC₅₀ = 0.52 μM)²⁹ bound to *E. coli* FabI in the presence of NAD⁺. The results show that **5** is bound in the active site (Figure 2). The indole subunit binds in a lipophilic pocket and appears to interact with the aryl rings of two tyrosines, Tyr 146 and Tyr 156, and one phenylalanine, Phe 203, from the enzyme. The linking amide exists in a *cis* conformation and π -stacks over the nicotinamide ring of the NAD⁺ cofactor. The carbonyl of the amide interacts with the hydroxyl of Tyr 156 from the enzyme as well as with the ribose 2'-hydroxyl from the cofactor. The 4-amino group is engaged in a hydrogen-bonding interaction with one of the phosphate groups of NAD⁺, and the benzylic amide may interact with the adenine group of NAD⁺ through a bound water molecule.

The mode of binding of **5** appears to be very similar to that of triclosan, a known FabI inhibitor.^{12–16} In the X-ray cocrystal structure of triclosan bound to *E. coli* FabI/NAD⁺,^{30–33} the phenolic aromatic ring π -stacks over the nicotinamide ring of the NAD⁺ cofactor, with the phenolic hydroxyl involved in hydrogen-bonding

Table 1. FabI Inhibition and Antibacterial Activity^a

Entry	Structure	FabI IC ₅₀ (μM)		MIC (μg/mL)	
		<i>S. aureus</i>	<i>H. influenzae</i>	<i>S. aureus</i>	<i>H. influenzae</i>
Triclosan		0.07 ± 0.05	NT	≤0.06	≤0.06
1		16.5 ± 2.4	6.9 ± 2.3	>64	>64
2		9.9 ± 2.8	5.1 ± 0.2	>64	>64
3		676 ± 123	>100	>64	>64
4		21.2 ± 5.1	2.5 ± 0.2	16	>64
5		6.7 ± 0.5	4.7 ± 0.3	16	>64
6		107 ± 34	121 ± 9	>64	>64
7		16.3 ± 3.4	2.6 ± 0.2	32	>64
8		>100	>100	>64	>64
9		2.4 ± 1.2	4.2 ± 1.1	0.5	>64
10		2.2 ± 0.3	4.3 ± 0.8	2	>64
11		93.7 ± 7.8	97.4 ± 7.4	>64	>64
12		>100	19.2 ± 3.3	>64	>64
13		11.2 ± 3.8	9.0 ± 2.2	32	>64
14		14.2 ± 5.3	15.2 ± 2.9	16	>64

^a Triclosan and compounds 1–14 have IC₅₀ > 30 μM vs *S. pneumoniae* FabK. Compounds 1–14 have MIC > 64 μg/mL vs *E. faecalis* and *S. pneumoniae*. Compound 9 has MIC = 8 μg/mL vs *E. coli* AcrAB⁻ and 4 μg/mL vs *M. catarrhalis*.

interactions with the hydroxyl of Tyr 156 from the enzyme as well as with the ribose 2'-hydroxyl from the cofactor. In support of this binding mode, kinetic studies^{32–34} have shown that triclosan forms a tight-

binding complex with FabI and NAD⁺. In the X-ray crystal structure, the phenol subunit of triclosan appears to function as a transition state enolate mimetic, taking the place of the enolate that results from hydride

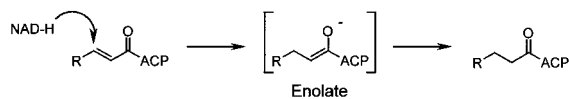


Figure 3. FabI-mediated reduction of enoyl-ACP.

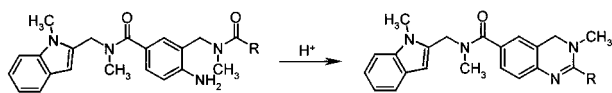


Figure 4. Cyclodehydration of *p*-aminobenzamide derivatives.

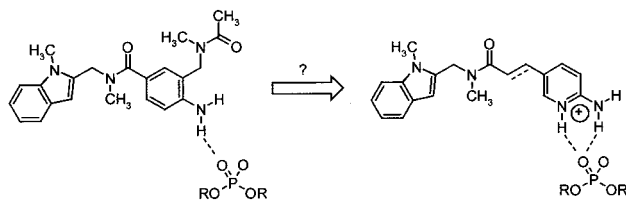


Figure 5. Design of aminopyridine-based FabI inhibitors.

delivery from the cofactor to the β -position of the natural substrate, crotonoyl-ACP (Figure 3). Since the linking amide in **5** is engaged in the same interactions as the phenol of triclosan, we speculate that this amide functions as a mimic of the transition-state enolate.³⁵

The X-ray crystal structure data suggested several interesting possibilities for optimization of **5**, but when we began to prepare derivatives in this series, we soon found that these compounds were susceptible to varying degrees of cyclodehydration, and the resultant dihydroquinazoline derivatives (Figure 4) were no longer FabI inhibitors (data not shown). Consequently, we turned our attention to the identification of compounds related to **5** that lacked this undesirable chemical instability.

Following consideration of the *S. aureus* FabI/NAD⁺ crystal structure and the previous SAR, we envisioned replacing the aniline moiety with an aminopyridine (Figure 5). We speculated that the amidine-like arrangement of nitrogens in an aminopyridine might provide a more favorable interaction with the key phosphate oxygen from the cofactor if the aminopyridine were to exist in a protonated form in the enzyme active site. (This turned out not to be the case; see below.) To maximize overlap with **5**, the pyridine subunit would be attached to the amide via a two-carbon linker, either saturated or unsaturated, depending on the need for rigidification. This would place the pyridine nitrogen of the new compound in a position similar to that of the aniline nitrogen of **5**. The acetylamino side chain of **5** might be mimicked by a substituent at the 3- or 4-position of the aminopyridine, but for simplicity, this substituent was left out of the original design. Compounds **9** and **11** became our initial targets and were prepared as described in Scheme 4.

Compound **9** was found to be a low micromolar inhibitor of FabI from *S. aureus* ($IC_{50} = 2.4 \mu M$) and *H. influenzae* ($IC_{50} = 4.2 \mu M$), with good antibacterial activity against *S. aureus* (MIC = 0.5 $\mu g/mL$), *M. catarrhalis* (MIC = 4 $\mu g/mL$), and the efflux mutant *E. coli* AcrAB⁻ (MIC = 8 $\mu g/mL$). However, **9** has $IC_{50} > 30 \mu M$ against *S. pneumoniae* FabK and consequently has MIC > 64 $\mu g/mL$ against the FabK-containing organisms *E. faecalis* and *S. pneumoniae*.⁷ The lack of a detectable MIC against *H. influenzae* may be due to efflux or poor penetration, since **9** has good activity

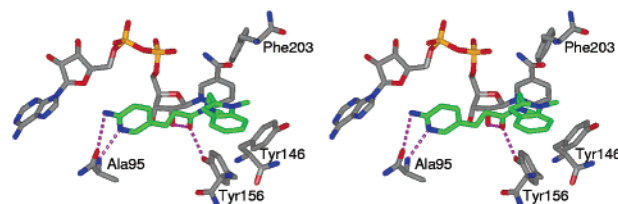


Figure 6. Representation of the X-ray crystal structure of **9** bound to *E. coli* FabI/NAD⁺.

against *H. influenzae* FabI. Importantly, the antibacterial activity of **9** does not appear to be due to a nonspecific cytotoxic or lytic effect ($IC_{50} = 512 \mu g/mL$ in an XTT assay using the human A549 lung cell line; $IC_{50} = 630 \mu M$ in a liposome lysis assay). In addition, **9** has no detectable activity against the human fatty acid biosynthesis enzyme ($IC_{50} > 100 \mu M$).

The level of antibacterial activity of **9** against *S. aureus* (MIC = 0.5 $\mu g/mL$) might appear to be better than expected on the basis of its level of activity against *S. aureus* FabI ($IC_{50} = 2.4 \mu M$, apparent $K_i = 0.21 \pm 0.11 \mu M$ ³⁶) and the relationship between IC_{50} values and MIC values for the other compounds tested. The reasons for this are not entirely clear at this time. However, we are confident that the antibacterial activity is not due to multiple mechanisms of action. Mechanism of action studies, described briefly below and in detail elsewhere,³⁷ suggest that the antibacterial activity of **9** is due to inhibition of fatty acid biosynthesis through inhibition of FabI. Furthermore, cytotoxicity studies suggest that the antibacterial activity is not due to a nonspecific cytotoxic effect (see above). Therefore, we speculate that compound **9** might have very good penetration in *S. aureus*, and this could account for the observed activity level. Alternatively, there is a possibility that FabI is more rate-limiting in *S. aureus* than in other organisms, thereby rendering *S. aureus* hypersensitive to FabI inhibitors. Clearly, additional investigation is required to accurately define the nature of the potent antibacterial activity of **9** against *S. aureus*.

A brief further investigation around **9** was conducted in an effort to confirm the key pharmacophore. The corresponding saturated derivative **11** and the compound without the two-carbon linker (**12**) are both much less potent, demonstrating the importance of the olefin. Derivatives lacking the pyridine nitrogen (**13**) or the 2-amino group (**14**) are also much less active, indicating that an intact 2-aminopyridine moiety is important for activity. The 2-aminopyrimidine **10**, which maintains the amidine-like character of a 2-aminopyridine, is well-tolerated by the enzyme but has lower levels of antibacterial activity. Taken together, these results suggest that an intact 3-(2-aminopyridinyl)acrylamide subunit is the minimum key pharmacophore for FabI activity as well as antibacterial activity.

The X-ray cocrystal structure of **9** (*E. coli* FabI $IC_{50} = 0.37 \mu M$)²⁹ with *E. coli* FabI/NAD⁺ reveals the key binding interactions. The crystal structure shows that **9** is bound in the active site (Figure 6), with the amide and indole subunits making the same contacts as in **5**. However, while the aminopyridine subunit of **9** binds in the same general region as the aminoaromatic of **5**, it does not bind in the proposed binding mode (Figure 5). Instead of interacting with the phosphate group via hydrogen bonds, the aminopyridine moiety is engaged

in two hydrogen-bonding interactions with Ala 95 from the protein. Presumably, the aminopyridine does not bind as expected because it does not appear to be protonated in the active site. As a result, the proposed bidentate-like interaction with the key phosphate oxygen of the cofactor cannot occur. In fact, the positioning of an unprotonated pyridine nitrogen in the proposed binding model (Figure 5) might be expected to destabilize the interaction with the phosphate oxygen via electrostatic repulsion. However, the unique arrangement of a hydrogen bond acceptor and a hydrogen bond donor present in the neutral aminopyridine species facilitates the observed interaction with a backbone amino acid residue within FabI. These unexpected results reveal an important new binding interaction between *E. coli* FabI/NAD⁺ and a small-molecule inhibitor. Consistent with this binding mode, enzymology studies show that **9** is not a substrate for FabI.³⁸

Further biological characterization of **9** is discussed in detail elsewhere.³⁷ Briefly, in mode of action studies, **9** exhibits elevated MICs against a FabI-overexpressing strain of *S. aureus*,^{16,37} suggesting that FabI is the primary antibacterial target. In addition, **9** selectively inhibits the incorporation of acetate in macromolecular synthesis (MMS) studies in *S. aureus*, indicating that the mode of action is via inhibition of fatty acid biosynthesis. Taken together, the overexpressor and MMS results suggest that the antibacterial mode of action of **9** is inhibition of fatty acid biosynthesis via inhibition of FabI. In in vivo studies, following intraperitoneal dosing at 50 mg/kg, **9** was found to be effective in a *S. aureus* groin abscess infection model in rats, providing an approximately 2.5 log reduction in bacterial counts relative to untreated controls.

Conclusion

We have described the identification of the aminopyridine derivative **9** as a novel small-molecule inhibitor of bacterial enoyl-ACP reductase (FabI). Compound **9** is a low micromolar inhibitor of FabI from *S. aureus* and *H. influenzae*, has good narrow-spectrum in vitro antibacterial activity, and is effective in vivo in a *S. aureus* infection model in rats. Mode of action and cytotoxicity studies confirm that the antibacterial activity of **9** is due to inhibition of fatty acid biosynthesis through inhibition of FabI. Furthermore, the compound is a selective inhibitor of bacterial FAS, showing no detectable inhibition of the human FAS system. These results demonstrate that FabI is a valid antibacterial target and that small-molecule FabI inhibitors have the potential to be systemically active agents for the treatment of bacterial infections. Further studies in this area are ongoing in our laboratories, and results will be reported in due course.

Experimental Section

All commercially available chemicals and solvents were used without further purification unless indicated otherwise. All new compounds gave satisfactory spectroscopic and/or analytical data. ¹H NMR spectra were recorded at 250, 300, 360, or 400 MHz, and chemical shifts are reported in parts per million (δ) downfield from the internal standard tetramethylsilane (TMS). Mass spectra were obtained using electrospray (ES) ionization techniques. Elemental analyses were performed by

Quantitative Technologies Inc., Whitehouse, NJ. Analtech Silica Gel GF and E. Merck Silica Gel 60 F-254 thin layer plates were used for thin-layer chromatography. Flash chromatography was carried out on E. Merck Kieselgel 60 (230–400 mesh) silica gel. Analytical HPLC was performed on Beckman chromatography systems. Preparative HPLC was performed using Gilson chromatography systems. ODS refers to an octadecylsilyl derivatized silica gel chromatographic support. YMC Combi Prep ODS-A is an ODS chromatographic support and is a registered trademark of YMC Co. Ltd., Kyoto, Japan. Celite is a filter aid composed of acid-washed diatomaceous silica and is a registered trademark of Manville Corp., Denver, CO.

1-Methyl-2-(methylaminomethyl)-1H-indole (23). A suspension of 1-methylindole-2-carboxaldehyde (5.0 g, 31.4 mmol) in 2.0 M methylamine/methanol (150 mL) was stirred for 24 h at room temperature and then was concentrated to dryness in vacuo. The remaining solid residue was taken up in ethanol (150 mL), and NaBH₄ (1.19 g, 31.4 mmol) was added with stirring at room temperature. Vigorous gas evolution was observed, which subsided after 15 min. The reaction mixture was stirred for 4 h, then was concentrated to dryness. The residue was treated with 1.0 N NaOH (150 mL) and extracted with Et₂O (150 mL). The combined organic layers were washed with brine, dried (Na₂SO₄), and concentrated to dryness to give **23** (5.39 g, 98%) as a yellow oil: ¹H NMR (400 MHz, CDCl₃) δ 7.56 (d, *J* = 7.8 Hz, 1H), 7.29 (d, *J* = 8.2 Hz, 1H), 7.19 (app t, 1H), 7.08 (app t, 1H), 6.39 (s, 1H), 3.90 (s, 2H), 3.77 (s, 3H), 2.50 (s, 3H), 1.44 (br s, 1H); MS (ES) *m/e* 175.0 (M + H)⁺.

(2R)-2-[(Carbomethoxy)methyl]-N,4-dimethyl-N-(1-methyl-1H-indol-2-ylmethyl)-3-oxo-2,3,4,5-tetrahydro-1H-1,4-benzodiazepine-7-carboxamide (2). To a solution of (2R)-2-[(carbomethoxy)methyl]-4-methyl-3-oxo-2,3,4,5-tetrahydro-1H-1,4-benzodiazepine-7-carboxylic acid²⁵ (0.4 g, 1.37 mmol) in dry DMF (10 mL) at room temperature was added **23** (0.26 g, 1.50 mmol), HOBT·H₂O (0.20 g, 1.50 mmol), *i*-Pr₂NEt (0.19 g, 1.50 mmol), and EDC (0.29 g, 1.50 mmol). After 18 h, the reaction solution was diluted with H₂O (25 mL) and extracted with EtOAc (2 × 50 mL). The organic fractions were combined, washed sequentially with H₂O and brine, and then dried (Na₂SO₄). Concentration in vacuo followed by chromatography on silica gel (95:5 CHCl₃/MeOH) provided **2** (0.56 g, 92%) as an off-white solid: ¹H NMR (300 MHz, CDCl₃) δ 7.60 (d, *J* = 7.7 Hz, 1H), 7.12–7.32 (m, 6H), 6.51 (m, 2H), 5.40 (d, *J* = 16.4 Hz, 1H), 5.06 (t, *J* = 7.7 Hz, 1H), 3.74–3.74 (m, 7H), 3.03 (s, 3H), 2.98 (s, 3H), 2.70 (dd, *J* = 12.8, 6.3 Hz, 1H); MS (ES) *m/e* 449 (M + H)⁺. Anal. (C₂₅H₂₈N₄O₄·0.75H₂O) C, H, N.

(2S)-2-[(Carbomethoxy)methyl]-N,4-dimethyl-N-(1-methyl-1H-indol-2-ylmethyl)-3-oxo-2,3,4,5-tetrahydro-1H-1,4-benzodiazepine-7-carboxamide (3). According to the procedure for the preparation of **2**, except substituting (2S)-2-[(carbomethoxy)methyl]-4-methyl-3-oxo-2,3,4,5-tetrahydro-1H-1,4-benzodiazepine-7-carboxylic acid^{24,25} (0.4 g, 1.37 mmol) for the (2R)-2-[(carbomethoxy)methyl]-4-methyl-3-oxo-2,3,4,5-tetrahydro-1H-1,4-benzodiazepine-7-carboxylic acid, **3** (0.56 g, 92%) was prepared as an off-white solid: MS (ES) *m/e* 449 (M + H)⁺; HRMS calcd for C₂₅H₂₈N₄O₄ 448.2111, found 448.2107.

tert-Butyl 4-Fluoro-3-methylbenzoate (16). To a stirred solution of di-*tert*-butyl dicarbonate (11 g, 50.4 mmol) in dry THF (50 mL) with stirring under argon at –78 °C was added over 5 min a 1.0 M solution of 4-fluoro-3-methylphenylmagnesium bromide in THF (**15**, 50 mL, 50 mmol). After 15 min, the cooling bath was removed and the reaction mixture was allowed to warm to room temperature. After 4 h at room temperature, the reaction mixture was concentrated to dryness in vacuo. The residue was taken up in Et₂O (250 mL) and washed sequentially with 1.0 N NaOH (250 mL) and brine (250 mL). Drying (MgSO₄) and concentration left an oil that was distilled through a short-path distillation apparatus under high vacuum. The fraction boiling at 92–95 °C (1 mmHg) was collected to give **16** (9.85 g, 94%) as a clear oil: ¹H NMR (300 MHz, CDCl₃) δ 7.78–7.85 (m, 2H), 7.02 (t, *J* = 1.8 Hz, 1H), 2.30 (d, *J* = 1.8 Hz, 3H), 1.59 (s, 9H); MS (ES) *m/e* 211.0 (M + H)⁺.

tert-Butyl 4-Fluoro-3-(methylaminomethyl)benzoate (18). A mixture of **16** (9.85 g, 46.9 mmol), *N*-bromosuccinimide (10 g, 56 mmol), benzoyl peroxide (0.6 g, 2.5 mmol), and CCl₄ (100 mL) was heated at reflux and irradiated with a 150 W tungsten flood lamp. After 24 h, the reaction mixture was cooled to room temperature and filtered, and the filter pad was washed with CCl₄ (25 mL). The filtrate was concentrated to give the crude benzylic bromide (**17**, 15.11 g, 59% pure by GC, containing 32% dibromide) as a yellow oil. To a solution of this crude bromide in THF (150 mL) was added with stirring at 0 °C a solution of methylamine (40 wt % in H₂O, 20 mL, 232 mmol) in one portion. The reaction mixture was allowed to warm to room temperature and was stirred for 18 h, then was concentrated to half its volume. The residue was diluted with H₂O (250 mL) and extracted with Et₂O (2 × 150 mL). The combined organic layers were washed sequentially with 1.0 N NaOH (150 mL) and brine (150 mL), dried (Na₂SO₄), and concentrated. The remaining residue was purified by flash chromatography on silica gel (10% MeOH in 1:1 EtOAc/CHCl₃) to give **18** (4.85 g, 43%) as a yellow oil: ¹H NMR (250 MHz, CDCl₃) δ 7.97 (dd, *J* = 7.3, 2.3 Hz, 1H), 7.90 (m, 1H), 7.07 (app t, 1H), 3.83 (s, 2H), 2.46 (s, 3H), 1.59 (s, 9H); MS (ES) *m/e* 240.0 (M + H)⁺.

tert-Butyl 3-[[[2-(Benzyloxycarbonylamino)acetyl]-methylamino]methyl]-4-fluorobenzoate (19). To a stirred solution of **18** (4.00 g, 16.7 mmol) in 1:1 DMF/CH₂Cl₂ (100 mL) was added *N*-(benzyloxycarbonyl)glycine (3.50 g, 16.7 mmol) and HOBt·H₂O (2.3 g, 17 mmol), followed by DCC (3.51 g, 17 mmol). The reaction mixture was stirred for 16 h and then was concentrated to dryness. Purification by flash chromatography on silica gel (30% EtOAc/hexanes) gave **19** (7.26 g, 100%) as a thick yellow oil: ¹H NMR (400 MHz, CDCl₃) δ 7.90–7.94 (m, 2H), 7.38–7.39 (m, 5H), 7.28 (m, 1H), 5.85 (br s, 1H), 5.15 (s, 2H), 4.70 (s, 2H), 4.10 (d, *J* = 3.9 Hz, 2H), 2.98 (s, 3H), 1.60 (s, 9H); MS (ES) *m/e* 431.02 (M + H)⁺.

tert-Butyl 4-Methyl-3-oxo-2,3,4,5-tetrahydro-1H-1,4-benzodiazepine-7-carboxylate (21). A mixture of **19** (7.2 g, 16.7 mmol), 10% Pd/C (3.0 g, 2.8 mmol), and MeOH (200 mL) was shaken at room temperature under H₂ (50 psi) on a Parr apparatus. After 4 h, the reaction mixture was filtered through Celite, and the filter pad was washed with MeOH. The filtrate was concentrated, and the remaining residue (crude **20**) was taken up in dry DMSO (75 mL). The solution was evacuated and purged with argon (3×), then was heated with stirring at 125 °C for 24 h. Most of the DMSO was removed by distillation under vacuum, and the remaining solution was diluted with EtOAc (100 mL). The solution was washed sequentially with saturated NaHCO₃ (100 mL) and brine (100 mL), dried (Na₂SO₄), and concentrated. The remaining residue was purified by flash chromatography on silica gel (80% EtOAc/hexanes) to give **21** (2.26 g, 48%) as a white solid: ¹H NMR (300 MHz, DMSO-*d*₆) δ 7.52 (s, 1H), 7.50 (dd, *J* = 8.9, 2.0 Hz, 1H), 6.95 (br s, 1H), 6.50 (d, *J* = 8.1 Hz, 1H), 4.61 (s, 2H), 4.08 (s, 2H), 2.92 (s, 3H), 1.51 (s, 9H); MS (ES) *m/e* 277.4 (M + H)⁺.

N,4-Dimethyl-N-(1-methyl-1H-indol-2-ylmethyl)-3-oxo-2,3,4,5-tetrahydro-1H-1,4-benzodiazepine-7-carboxamide (4). To a stirred solution of **21** (0.60 g, 2.2 mmol) in CH₂Cl₂ (25 mL) was added trifluoroacetic acid (25 mL). After being stirred at room temperature for 45 min, the reaction mixture was concentrated in vacuo. The residue was redissolved in 4 N HCl in dioxane (50 mL), and the solution was concentrated to dryness. Trituration with Et₂O, filtration, and drying under vacuum gave the crude carboxylic acid hydrochloride salt (**22**) as a white solid. To a stirred solution of this material in 1:1 DMF/CH₂Cl₂ (50 mL) was added **23** (0.35 g, 2.2 mmol), Et₃N (0.62 mL, 4.4 mmol), HOBt·H₂O (0.30 g, 2.2 mmol), and EDC·HCl (0.42 g, 2.2 mmol). After being stirred for 18 h, the reaction mixture was concentrated in vacuo and the residue was taken up in EtOAc (50 mL). The solution was washed sequentially with H₂O (50 mL), 1.0 N Na₂CO₃ (50 mL), and brine (50 mL), then was dried (Na₂SO₄) and concentrated. Purification by flash chromatography on silica gel (5% MeOH/CHCl₃) gave **4** (0.76 g, 92%) as an off-white solid: ¹H NMR

(300 MHz, DMSO-*d*₆) δ 7.51 (d, *J* = 7.8 Hz, 1H), 7.42 (d, *J* = 8.1 Hz, 1H), 7.13–7.18 (m, 3H), 7.02 (app t, 1H), 6.61 (br s, 1H), 6.47 (d, *J* = 8.2 Hz, 1H), 6.44 (s, 1H), 4.83 (s, 2H), 4.58 (s, 2H), 4.04 (s, 2H), 3.66 (s, 3H), 2.92 (s, 3H), 2.89 (s, 3H); MS (ES) *m/e* 377.0 (M + H)⁺; HRMS calcd for C₂₂H₂₄N₄O₂ 376.1899, found 376.1896.

tert-Butyl 3-Methyl-4-nitrobenzoate (25). To a pyridine solution of 3-methyl-4-nitrobenzoic acid (**24**, 18.1 g, 100.0 mmol) at room temperature was added benzenesulfonyl chloride in one portion. After 10 min, anhydrous *tert*-butyl alcohol (9.4 mL, 100.0 mmol) was added and the reaction mixture was allowed to stir for 1 h. The resulting suspension was poured into ice-water (400 mL) and stirred vigorously for 1 h. The light-yellow suspension was filtered through a sintered-glass funnel, and the filter cake was washed with H₂O. The resulting yellow solid was dissolved in toluene (400 mL), and the solution was dried over MgSO₄. The MgSO₄-containing mixture was filtered through a short column of silica gel, and the column was washed with toluene. Concentration of the filtrate in vacuo followed by drying in high vacuum afforded **25** (22.5 g, 95%) as a light-yellow solid: ¹H NMR (250 MHz, CDCl₃) δ 7.85–8.10 (m, 3H), 2.61 (s, 3H), 1.60 (s, 9H); MS (ES) *m/e* 238 (M + H)⁺.

tert-Butyl 3-(Methylaminomethyl)-4-nitrobenzoate (27). To a stirred solution of **25** (22.5 g, 94.9 mmol) in CH₂Cl₂ (450 mL) in a 1 L round-bottom flask at room temperature was added NBS (18.6 g, 104.4 mmol) and benzoyl peroxide (2.3 g, 9.5 mmol). The flask was equipped with a reflux condenser, and a 150 W tungsten light source irradiated the reaction mixture. After 36 h, the reaction solution was cooled to room temperature, washed with H₂O, dried over Na₂SO₄, and concentrated in vacuo. The resulting orange residue was dissolved in ethyl acetate and filtered through silica gel (1:4 EtOAc/hexanes). Concentration in vacuo gave the crude bromide (**26**) as an orange oil. This was used without further purification.

To the crude bromide (**26**) in THF (150 mL) was added 40% aqueous CH₃NH₂ (50 mL) in one portion at room temperature. After 18 h, the reaction solution was concentrated to remove the THF. The resulting aqueous solution was extracted with EtOAc (2 × 200 mL), and the combined organic phases were washed sequentially with H₂O and brine. Drying over K₂CO₃ and concentration gave a yellow oil. Purification by flash chromatography on silica gel (1:1 hexanes/EtOAc) gave **27** (19.2 g, 76%) as a light-yellow solid: MS (ES) *m/e* 267 (M + H)⁺.

tert-Butyl 3-[(*N*-Acetyl-*N*-methylamino)methyl]-4-aminobenzoate (29). To a stirred solution of **27** (2.4 g, 9.0 mmol) in CH₂Cl₂ at room temperature was added Et₃N (2.52 mL, 18.0 mmol) and acetic anhydride (1.8 g, 18.0 mmol). After 12 h, the reaction mixture was concentrated in vacuo and the residue was dissolved in EtOAc (150 mL). The solution was washed with H₂O, dried over Na₂SO₄, and concentrated in vacuo to afford the acetylated derivative (**28**) as a yellow oil. This was further dried under high vacuum and then was used directly in the next step.

The crude acetyl derivative (**28**) was dissolved in EtOAc (50 mL) and CH₃OH (50 mL) in a Parr hydrogenation flask. A catalytic amount of 10% Pd/C was added to the solution, and the reaction mixture was shaken on a Parr shaker under H₂ (50 psi) for 4 h. The resulting mixture was filtered through Celite, and the filtrate was concentrated in vacuo. Purification by flash chromatography on silica (1:1 EtOAc/hexanes) gave **29** (2.13 g, 85% over two steps) as an off-white solid: ¹H NMR (400 MHz, DMSO-*d*₆) δ 7.72 (m, 2H), 6.57 (d, *J* = 8.1 Hz, 1H), 5.12 (br s, 2H), 4.49 (s, 2H), 2.92 (s, 3H), 2.11 (s, 3H), 1.58 (s, 9H); MS (ES) *m/e* 279 (M + H)⁺.

3-[(*N*-Acetyl-*N*-methylamino)methyl]-4-aminobenzoic Acid, Trifluoroacetate Salt (30). To a solution of **29** (2.13 g, 7.65 mmol) in CH₂Cl₂ (150 mL) at room temperature was added TFA (30 mL). After 12 h, the reaction mixture was concentrated to an oil and dried under high vacuum overnight. The resulting residue was washed with hexanes and Et₂O to afford **30** (2.56 g, 7.60 mmol) as an off-white solid: ¹H NMR

(400 MHz, DMSO- d_6) δ 7.62 (m, 2H), 6.60 (d, J = 8.3 Hz, 1H), 6.05 (m, 2H), 4.36 (m, 2H), 2.87 (s, 3H), 2.06 (s, 3H); MS (ES) m/e 223 (M + H)⁺.

3-[(N-Acetyl-N-methylamino)methyl]-4-amino-N-methyl-N-(1-methyl-1H-indol-2-ylmethyl)benzamide (5). To a stirred solution of **30** (0.73 g, 2.17 mmol) in DMF (20 mL) at room temperature was added diisopropylethylamine (0.83 mL, 4.78 mmol), HOBt-H₂O (0.32 g, 2.39 mmol), and **23** (0.40 g, 2.39 mmol), followed by EDC (0.45 g, 2.39 mmol). After 12 h, the reaction mixture was poured onto H₂O (100 mL) and extracted with EtOAc (2 \times 100 mL). The organic phases were combined and washed sequentially with H₂O (100 mL) and brine. Drying over Na₂SO₄ and purification by flash chromatography on silica gel (5:95 CH₃OH/CHCl₃) gave **5** (0.73 g, 89%) as a light-yellow solid: ¹H NMR (300 MHz, CDCl₃) δ 7.25 (d, J = 7.7 Hz, 1H), 7.15 (d, J = 7.7 Hz, 1H), 6.96 (m, 2H), 6.93 (t, J = 7.2 Hz, 1H), 6.77 (t, J = 7.2 Hz, 1H), 6.35 (d, J = 8.8 Hz, 1H), 6.18 (s, 1H), 4.56 (s, 2H), 4.05 (s, 2H), 3.38 (s, 3H), 3.14 (s, 3H), 2.68 (s, 3H), 1.70 (s, 3H); MS (ES) m/e 379 (M + H)⁺; HRMS calcd for C₂₂H₂₆N₄O₂ 378.2056, found 378.2055.

3-[(N-Acetyl-N-methylamino)methyl]benzoic Acid (33). A solution of 3-chloromethylbenzoic acid (**31**, 1.0 g, 5.86 mmol) in 2 M methylamine/methanol (100 mL) was stirred at 50 °C for 16 h, then was concentrated in vacuo. The residue was re-concentrated twice from methanol, then was taken up in CHCl₃ (100 mL) at room temperature. Et₃N (2.5 mL, 17.9 mmol) was added, followed by Ac₂O (1.1 mL, 11.7 mmol). The reaction was exothermic. After 3 h, the reaction mixture was concentrated in vacuo and the residue was taken up in EtOAc. The solution was washed with 1 N HCl and then with brine, dried (MgSO₄), and concentrated to dryness. Trituration with Et₂O, filtration, and drying under vacuum gave **33** (0.65 g, 53%) as a white crystalline solid: ¹H NMR (300 MHz, DMSO- d_6) δ 13.02 (br s, 1H), 7.76–7.86 (m, 2H), 7.46–7.53 (m, 2H), 7.55 (s, 2H), 2.92 (s, 3H), 2.08 (s, 3H); MS (ES) m/e 207.9 (M + H)⁺.

3-[(N-Acetyl-N-methylamino)methyl]-N-methyl-N-(1-methyl-1H-indol-2-ylmethyl)benzamide (6). To a solution of **33** (0.5 g, 2.4 mmol) in 1:1 DMF/CH₂Cl₂ (50 mL) was added **23** (0.40 g, 2.5 mmol), Et₃N (0.35 mL, 2.5 mmol), HOBt-H₂O (0.34 g, 2.5 mmol), and EDC (0.48 g, 2.5 mmol). After being stirred at room temperature for 16 h, the reaction mixture was concentrated in vacuo and the residue was taken up in EtOAc. The solution was washed with 1 N HCl and then with brine, dried (MgSO₄), and concentrated to dryness. Purification by flash chromatography on silica gel (5% EtOH/EtOAc) gave **6** (0.75 g, 86%) as an off-white solid: ¹H NMR (400 MHz, DMSO- d_6) δ 7.53 (d, J = 7.8 Hz, 1H), 7.40–7.43 (m, 2H), 7.36 (app t, 1H), 7.29 (d, J = 8.2 Hz, 1H), 7.14 (app t, 1H), 7.03 (app t, 1H), 6.49 (s, 1H), 4.91 (s, 2H), 4.52 (s, 2H), 3.75 (s, 3H), 2.92 (s, 3H), 2.83 (s, 3H), 2.07 (s, 3H); MS (ES) m/e 364.4 (M + H)⁺; HRMS calcd for C₂₂H₂₅N₃O₂ 363.1947, found 363.1943.

4-Amino-N-methyl-N-(1-methyl-1H-indol-2-ylmethyl)benzamide (7). According to the procedure for the preparation of **5**, except substituting 4-aminobenzoic acid (0.50 g, 3.65 mmol) for **30**, compound **7** (1.0 g, 93%) was prepared as an off-white solid: ¹H NMR (400 MHz, CDCl₃) δ 7.60 (d, J = 7.8 Hz, 1H), 7.21–7.45 (m, 4H), 7.13 (t, J = 7.0 Hz, 1H), 6.64 (d, J = 8.4 Hz, 2H), 6.50 (s, 1H), 4.88 (s, 2H), 3.86 (s, 3H), 2.88 (s, 3H); MS (ES) m/e 294 (M + H)⁺; HRMS calcd for C₁₈H₁₉N₃O 293.1528, found 293.1529.

N-Methyl-N-(1-methyl-1H-indol-2-ylmethyl)benzamide (8). According to the procedure for the preparation of **5**, except substituting benzoic acid (0.47 g, 3.85 mmol) for **30**, compound **8** (0.88 g, 91%) was prepared as an off-white solid: ¹H NMR (300 MHz, CDCl₃) δ 7.60 (d, J = 7.8 Hz, 1H), 7.21–7.45 (m, 2H), 7.13 (t, J = 6.9 Hz, 1H), 6.52 (s, 1H), 4.99 (s, 2H), 3.82 (s, 3H), 2.88 (s, 3H); MS (ES) m/e 279 (M + H)⁺. Anal. (C₁₈H₁₈N₂O) C, H, N.

Benzyl 3-(6-Aminopyridin-3-yl)acrylate (35a). A solution of 2-amino-5-bromopyridine (**34a**, 2.25 g, 13.0 mmol), benzyl acrylate (3.2 g, 19.7 mmol), Pd(OAc)₂ (0.31 g, 1.4 mmol), tri-*o*-tolylphosphine (0.73 g, 2.4 mmol), and diisopropylethyl-

amine (3.5 mL, 20.0 mmol) in propionitrile (50 mL) was heated at reflux overnight. The dark mixture was filtered through Celite, and the filtrate was concentrated. Flash chromatography on silica gel (3% MeOH/CH₂Cl₂) gave **35a** (1.3 g, 39%): ¹H NMR (300 MHz, CDCl₃) δ 8.19 (d, J = 2.3 Hz, 1H), 7.64 (dd, J = 8.6, 2.3 Hz, 1H), 7.62 (d, J = 16.0 Hz, 1H), 7.25–7.50 (m, 5H), 6.50 (d, J = 8.6 Hz, 1H), 6.30 (d, J = 16.0 Hz, 1H), 5.24 (s, 2H), 4.77 (br s, 2H); MS (ES) m/e 255 (M + H)⁺.

3-(6-Aminopyridin-3-yl)acrylic Acid (36a). A solution of **35a** (1.3 g, 5.1 mmol) and 1.0 N NaOH (10 mL, 10 mmol) in MeOH was heated at reflux overnight. The solution was concentrated in vacuo, and the residue was dissolved in H₂O. The pH was adjusted to 6 with dilute HCl, and the solid precipitate was collected by suction filtration and dried to give **36a** (0.6 g, 72%) as a white solid: MS (ES) m/e 165 (M + H)⁺.

3-(6-Aminopyridin-3-yl)acrylic Acid (36a). Alternative Preparation. Acrylic acid (23 mL, 0.33 mol) was added carefully to a solution of 2-amino-5-bromopyridine (**34a**, 25.92 g, 0.15 mole) and Na₂CO₃ (55.64 g, 0.53 mol) in H₂O (600 mL). PdCl₂ (0.53 g, 0.003 mol) was then added, and the mixture was heated at reflux. After 24 h, the reaction mixture was cooled to room temperature and filtered, and the filtrate was adjusted to pH 6 with aqueous HCl. Additional H₂O (0.5 L) was added to improve mixing, and the mixture was stirred for 1 h. The pH was readjusted to 6, then the solid was collected by suction filtration. The filter pad was washed sequentially with H₂O (2 \times 0.5 L), cold absolute EtOH (100 mL), and Et₂O (2 \times 250 mL). Drying in high vacuum at elevated temperature gave **36a** (15.38 g, 62%) as a tan solid: ¹H NMR (300 MHz, DMSO- d_6) δ 8.11 (d, J = 2.0 Hz, 1H), 7.75 (dd, J = 8.7, 2.0 Hz, 1H), 7.43 (d, J = 15.8 Hz, 1H), 6.53 (s, 2H), 6.45 (d, J = 8.7 Hz, 1H), 6.22 (d, J = 15.8 Hz, 1H); MS (ES) m/e 165 (M + H)⁺.

3-(6-Aminopyridin-3-yl)-N-methyl-N-[(1-methyl-1H-indol-2-yl)methyl]acrylamide (9). EDC (0.70 g, 3.7 mmol) was added to a solution of **36a** (0.61 g, 3.7 mmol), **23** (0.65 g, 3.7 mmol), HOBt-H₂O (0.50 g, 3.7 mmol), and triethylamine (0.52 mL, 3.7 mmol) in DMF (30 mL) at room temperature. The reaction mixture was stirred overnight, then was concentrated in vacuo. The residue was diluted with 5% NaHCO₃ and extracted with CH₂Cl₂. The combined organic extracts were washed with brine and dried over MgSO₄. Flash chromatography on silica gel (3% MeOH/CH₂Cl₂) gave a colorless semisolid that was triturated with Et₂O and dried to afford **9** (1.0 g, 83%) as a white solid: ¹H NMR (300 MHz, CDCl₃) δ 8.20 (br s, 1H), 7.45–7.70 (m, 3H), 7.00–7.30 (m, 3H), 6.69 (d, J = 15.4 Hz, 1H), 6.30–6.50 (m, 2H), 4.89 (s, 2H), 4.67 (br s, 2H), 3.68 (s, 3H), 3.01 (s, 3H); MS (ES) m/e 321 (M + H)⁺. Anal. (C₁₉H₂₀N₄O \cdot 0.40H₂O) C, H, N.

Benzyl (E)-3-(2-Aminopyrimidin-5-yl)acrylate (35b). According to the procedure for the preparation of **35a**, except substituting 5-bromo-2-aminopyrimidine (**34b**, 1.95 g, 11.2 mmol) for **34a**, compound **35b** (2.25 g, 79%) was prepared as a light-orange solid: MS (ES) m/e 256 (M + H)⁺.

(E)-3-(2-Aminopyrimidin-5-yl)acrylic Acid (36b). According to the procedure for the preparation of **36a** (saponification method), except substituting **35b** (2.93 g, 11.5 mmol) for **35a**, compound **36b** (1.71 g, 90%) was prepared as an off-white solid: MS (ES) m/e 166 (M + H)⁺.

(E)-3-(2-Aminopyrimidin-5-yl)-N-methyl-N-(1-methyl-1H-indol-2-ylmethyl)acrylamide (10). According to the procedure for the preparation of **9**, except substituting **36b** (0.50 g, 3.0 mmol) for **36a**, compound **10** (0.86 g, 89%) was prepared as an off-white solid: ¹H NMR (400 MHz, DMSO- d_6) δ 8.64 (s, 2H), 7.41–7.52 (m, 3H), 6.99–7.12 (m, 3H), 6.35 (s, 1H), 4.83 (s, 2H), 3.70 (s, 3H), 3.11 (s, 3H); MS (ES) m/e 322 (M + H)⁺. Anal. (C₁₈H₁₉N₅O \cdot 0.5H₂O) C, H, N.

3-(6-Aminopyridin-3-yl)propionic Acid (38). Magnesium turnings (0.345 g, 14.2 mmol) were added to a solution of **35a** (0.72 g, 2.83 mmol) in dry MeOH (75 mL) at room temperature. The reaction mixture was stirred overnight, then was concentrated in vacuo. The residue was diluted with 10% HCl, and the aqueous layer was extracted with Et₂O. The Et₂O extracts

were discarded. The aqueous layer was basified to pH 10 with 1.0 N NaOH and extracted with Et₂O. The combined organic layers were washed with brine (3 × 10 mL), dried over MgSO₄, and concentrated to afford crude **37** (0.60 g) as a mixture of benzyl and methyl esters: MS (ES) *m/e* 181 (M + H)⁺ for methyl ester, 257 (M + H)⁺ for benzyl ester. The mixture was used without further purification.

A solution of crude **37** (0.60 g) and 1.0 N NaOH in MeOH was heated at reflux overnight, then was concentrated to dryness in vacuo. The residue was diluted with H₂O, and the mixture was extracted with Et₂O. The Et₂O extracts were discarded. The aqueous layer was acidified to pH 6 with dilute HCl. The precipitated solid was collected and dried to afford **38** (0.38 g, 83% for two steps) as a white solid: ¹H NMR (300 MHz, DMSO-*d*₆) δ 7.75 (br s, 1H), 7.19–7.25 (m, 1H), 6.40–6.51 (m, 1H), 6.37 (d, *J* = 8.5 Hz, 1H), 5.65 (br s, 2H), 2.50–2.68 (m, 2H), 2.25–2.50 (m, 2H); MS (ES) *m/e* 167 (M + H)⁺.

3-(6-Aminopyridin-3-yl)-*N*-methyl-*N*-(1-methyl-1*H*-indol-2-yl)methyl]propionamide (11). According to the procedure for the preparation of **9**, except substituting **38** (0.20 g, 1.14 mmol) for **36a**, compound **11** (18 mg, 5%) was prepared as an off-white solid following flash chromatography on silica gel (3% MeOH/CH₂Cl₂, two times) followed by preparative TLC (5% MeOH/CH₂Cl₂): ¹H NMR (360 MHz, DMSO-*d*₆, 330 K) δ 7.77 (br s, 1H), 7.46 (d, *J* = 8 Hz, 1H), 7.35 (d, *J* = 8 Hz, 1H), 7.17–7.27 (m, 1H), 7.03–7.12 (m, 1H), 6.92–7.01 (m, 1H), 6.38 (d, *J* = 8 Hz, 1H), 6.26 (br s, 1H), 5.29 (br s, 2H), 4.71 (s, 2H), 3.60 (s, 3H), 2.87 (s, 3H), 2.65–2.77 (m, 2H), 2.56–2.65 (m, 2H); MS (ES) *m/e* 323 (M + H)⁺. Anal. (C₁₉H₂₂N₄O·0.55H₂O) C, H, N.

6-Amino-*N*-methyl-*N*-(1-methyl-1*H*-indol-2-yl)nicotinamide (12). To a stirred solution of 6-aminonicotinic acid (0.35 g, 2.5 mmol) in 1:1 DMF/CH₂Cl₂ (30 mL) was added 1-methyl-2-(methylaminomethyl)-1*H*-indole (0.40 g, 2.5 mmol), Et₃N (0.35 mL, 2.5 mmol), HOBT·H₂O (0.34 g, 2.5 mmol), and EDC (0.48 g, 2.5 mmol). After being stirred for 16 h, the reaction mixture was concentrated in vacuo. Purification by flash chromatography on silica gel (5% MeOH/CHCl₃) gave **12** (520 mg, 72%) as an off-white solid: ¹H NMR (400 MHz, DMSO-*d*₆) δ 8.11 (d, *J* = 2.0 Hz, 1H), 7.54 (m, 2H), 7.43 (d, *J* = 8.2 Hz, 1H), 7.14 (app t, 1H), 7.03 (app t, 1H), 6.44 (s, 2H), 6.41 (s, 2H), 4.84 (s, 2H), 3.66 (s, 3H), 2.95 (s, 3H); MS (ES) *m/e* 294.9 (M + H)⁺; HRMS calcd for C₁₇H₁₈N₄O 294.1481, found 294.1483.

(*E*)-3-(4-Aminophenyl)-*N*-methyl-*N*-(1-methyl-1*H*-indol-2-ylmethyl)acrylamide (13). EDC (218 mg, 1.14 mmol) was added to a solution of 4-aminocinnamic acid hydrochloride (220 mg, 1.10 mmol), **23** (0.20 g, 1.15 mmol), HOBT·H₂O (154 mg, 1.14 mmol), and triethylamine (0.20 mL, 1.43 mmol) in DMF (20 mL) at room temperature. The reaction mixture was stirred overnight, then was concentrated in vacuo. The residue was diluted with 5% NaHCO₃ and extracted with CH₂Cl₂. The combined organic extracts were washed with brine (2 × 30 mL) and dried over MgSO₄. Flash chromatography on silica gel (3% MeOH/CH₂Cl₂) gave **13** (68 mg, 19%) as a yellow foam: ¹H NMR (360 MHz, DMSO-*d*₆, 330 K) δ 7.46 (d, *J* = 7.8 Hz, 1H), 7.42 (d, *J* = 15.3 Hz, 1H), 7.37 (d, *J* = 8.3 Hz, 1H), 7.32 (d, *J* = 8.5 Hz, 2H), 7.06–7.15 (m, 1H), 6.94–7.03 (m, 1H), 6.81 (d, *J* = 15.3 Hz, 1H), 6.58 (d, *J* = 8.5 Hz, 2H), 6.33 (s, 1H), 5.25 (br s, 2H), 4.85 (s, 2H), 3.70 (s, 3H), 3.02 (s, 3H); MS (ES) *m/e* 320 (M + H)⁺. Anal. (C₂₀H₂₁N₃O·0.20H₂O) C, H, N.

(*E*)-*N*-Methyl-*N*-(1-methyl-1*H*-indol-2-ylmethyl)-3-(pyridin-3-yl)acrylamide (14). EDC (0.22 g, 1.14 mmol) was added to a solution of *trans*-3-(3-pyridyl)acrylic acid (0.17 g, 1.14 mmol), **23** (0.20 g, 1.15 mmol), and HOBT·H₂O (0.15 g, 1.11 mmol) in DMF (10 mL) at room temperature. The reaction mixture was stirred overnight, then was concentrated in vacuo. The residue was diluted with 5% NaHCO₃ and extracted with CH₂Cl₂. The combined organic extracts were washed with brine and dried over MgSO₄. Flash chromatography on silica gel (3% MeOH/CH₂Cl₂) followed by preparative TLC (3% MeOH/CH₂Cl₂) gave **14** (0.14 g, 40%) as a white solid. ¹H NMR (360 MHz, CDCl₃) indicated an approximately 8:1 mixture of

amide rotamers; for the major rotamer: δ 8.79 (s, 1H), 8.59 (d, *J* = 3.9 Hz, 1H), 7.84 (d, *J* = 7.6 Hz, 1H), 7.76 (d, *J* = 15.5 Hz, 1H), 7.59 (d, *J* = 7.8 Hz, 1H), 7.38–7.48 (m, 2H), 7.19–7.27 (m, 1H), 7.08–7.17 (m, 1H), 6.98 (d, *J* = 15.5 Hz, 1H), 6.51 (s, 1H), 4.94 (s, 2H), 3.73 (s, 3H), 3.09 (s, 3H). MS (ES) *m/e* 306 (M + H)⁺. Anal. (C₁₉H₁₉N₃O·0.20H₂O) C, H, N.

X-ray Crystallography. Crystals of the *E. coli* FabI/NAD⁺ inhibitor complexes were obtained using the same methods and conditions as those reported earlier.³¹ Diffraction data to 2.4 Å resolution were collected at the Brookhaven National Laboratory. The structures were solved with the difference Fourier methods using the *E. coli* FabI/NAD⁺ triclosan structure³¹ as the starting model. The **5** cocrystal structure was refined with the program XPLOR,³⁹ while the **9** cocrystal structure was refined with the program CNX.⁴⁰ In both cases, 5% of the data were set aside for *R*_{free} calculations. There is one FabI dimer per crystalline asymmetric unit, with two molecules of inhibitor and two molecules of NAD⁺ bound. The flipping loop³¹ is disordered in both the **5** structure (193–205/193–202) and the **9** structure (197–202/196–201). The structures have good quality as indicated by various statistical measures as well as good quality electron density maps (see Supporting Information). The coordinates have been deposited in the Protein Databank for **5** (PDB accession code 1LX6) and **9** (PDB accession code 1LXC).

Enzyme Inhibition Assays. Assays were carried out in half-area 96-well microtiter plates. Compounds were evaluated in 150 μL (FabI) or 100 μL (FabK) assay mixtures containing components specific for each enzyme (see below). Inhibitors were typically varied over the range 0.01–10 μM. The consumption of NAD(P)H was monitored for 20 min at 30 °C by following the change in absorbance at 340 nm. IC₅₀ values were estimated from a fit of the initial velocities to a standard four-parameter model (eq 1), or variations thereof, and were

$$v = \frac{\text{range}}{\left(1 + \frac{[I]}{\text{IC}_{50}}\right)^s} + \text{background} \quad (1)$$

typically reported as the mean ± SD of duplicate determinations. A proprietary lead compound was included in all plates as a positive control.

S. aureus FabI assays contained 100 mM NaADA (ADA = *N*-[2-acetamido]-2-iminodiacetic acid), pH 6.5, 4% glycerol, 25 μM crotonoyl-ACP, 50 μM NADPH, and an appropriate dilution of *S. aureus* FabI (approximately 20 nM). Initial velocities were estimated from the slope of a linear fit of the progress curves.

H. influenzae FabI assays contained MDTG buffer (100 mM MES, 51 mM diethanolamine, 51 mM triethanolamine, pH 6.5 [MES = 2-(*N*-morpholino)ethanesulfonic acid], 4% glycerol), 25 μM crotonoyl-ACP, 50 μM NADH, and 9 nM *H. influenzae* FabI. Initial velocities were estimated from an exponential fit of the nonlinear progress curves and are equal to the slope of the tangent at *t* = 0 min.

E. coli FabI assays contained 100 mM NaADA, pH 6.5 (ADA = *N*-[2-acetamido]-2-iminodiacetic acid), 4% glycerol, 0.25 mM crotonoyl-CoA, 50 μM NADH, and approximately 60 nM *E. coli* FabI. Initial velocities were determined as above for *H. influenzae* FabI.

S. pneumoniae FabK assays contained MDTG buffer, pH 7.5, 100 mM NH₄Cl, 25 μM crotonoyl-ACP, 50 μM NADH, and 1.5 nM *S. pneumoniae* FabK. Initial velocities were determined as above for *H. influenzae* FabI.

Antimicrobial Activity Assay. Whole-cell antimicrobial activity was determined by broth microdilution. Test compounds were dissolved in DMSO and diluted 1:10 in water to produce a 256 μg/mL stock solution. By use of a 96-well microtiter plate, a Microlab AT Plus 2 (Hamilton Co., Reno, NV) serially diluted 50 μL of the stock solution into cation-adjusted Mueller Hinton broth (Becton Dickinson, Cockeysville, MD). After the compounds were diluted, a 50 μL aliquot of the test isolate (approximately × 10⁶ cfu/mL) was added to each well of the microtiter plate. The final test

concentrations ranged from 0.06 to 64 $\mu\text{g}/\text{mL}$. Inoculated plates were incubated at 35 °C in ambient air for 18–24 h. The minimum inhibitory concentration (MIC) was determined as the lowest concentration of compound that inhibited visible growth.

Acknowledgment. We thank the following GSK personnel for their contributions to this work: John Broskey and Leroy L. Voelker for cytotoxicity data, Robert I. Jepras for liposome lysis data, Priscilla H. Offen for NMR studies, Stone D. Shi and Mark E. Hemling for high-resolution mass spectra, and Ward W. Smith for preparing X-ray density figures and for depositing the X-ray crystallography data in the Protein Data Bank. We also thank the staff at beamline X12-C of the Biology Department Single-Crystal Diffraction Facility at the National Synchrotron Light Source (NSLS) of Brookhaven National Laboratory. The NSLS facility is supported by the U.S. Department of Energy, Offices of Health and Environmental Research and of Basic Energy Sciences under Contract DE-AC02-98CH10886, by the National Science Foundation, and by National Institutes of Health Grant 1P41 RR12408-01A1.

Supporting Information Available: A table of crystallographic data acquisition and refinement statistics for inhibitors **5** and **9** bound to *E. coli* FabI/NAD⁺ and density figures for inhibitors **5** and **9** bound to *E. coli* FabI/NAD⁺. This material is available free of charge via the Internet at <http://pubs.acs.org>.

References

- Alekshun, M. N.; Levy, S. B. Bacterial drug resistance: response to survival threats. In *Bacterial Stress Responses*; Storz, G., Hengge-Aronis, R., Eds.; ASM Press: Washington, DC, 2000; pp 323–366.
- Bax, R.; Mullan, N.; Verhoef, J. The millennium bugs—the need for and development of new antibacterials. *Int. J. Antimicrob. Agents* **2000**, *16*, 51–59.
- Setti, E. L.; Quattrocchio, L.; Micetich, R. G. Current approaches to overcome bacterial resistance. *Drugs Future* **1997**, *22*, 271–284.
- Chu, D. T. W.; Plattner, J. J.; Katz, L. New directions in antibacterial research. *J. Med. Chem.* **1996**, *39*, 3853–3874.
- For recent reviews of bacterial fatty acid biosynthesis as an antibacterial target, see the following: (a) Payne, D. J.; Warren, P. V.; Holmes, D. J.; Ji, Y.; Lonsdale, J. T. Bacterial fatty acid biosynthesis: a genomics driven target for antibacterial drug discovery. *Drug Discovery Today* **2001**, *6*, 537–544. (b) Heath, R. J.; White, S. W.; Rock, C. O. Lipid biosynthesis as a target for antibacterial agents. *Prog. Lipid Res.* **2001**, *40*, 467–497. (c) Campbell, J. W.; Cronan, J. E., Jr. Bacterial fatty acid biosynthesis: targets for antibacterial drug discovery. *Annu. Rev. Microbiol.* **2001**, *55*, 305–332.
- Heath, R. J.; Rock, C. O. Enoyl-acyl carrier protein reductase (*fabI*) plays a determinant role in completing cycles of fatty acid elongation in *Escherichia coli*. *J. Biol. Chem.* **1995**, *270*, 26538–26542.
- Heath, R. J.; Rock, C. O. A triclosan-resistant bacterial enzyme. *Nature* **2000**, *406*, 145.
- Bergler, H.; Fuchsichler, S.; Högenauer, G.; Turnowsky, F. The enoyl-[acyl-carrier-protein] reductase (FabI) of *Escherichia coli*, which catalyzes a key regulatory step in fatty acid biosynthesis, accepts NADH and NADPH as cofactors and is inhibited by palmitoyl-CoA. *Eur. J. Biochem.* **1996**, *242*, 689–694.
- Heath, R. J.; Li, J.; Roland, G. E.; Rock, C. O. Inhibition of the *Staphylococcus aureus* NADPH-dependent enoyl-acyl carrier protein reductase by triclosan and hexachlorophene. *J. Biol. Chem.* **2000**, *275*, 4654–4659.
- Baldock, C.; Rafferty, J. B.; Sedelnikova, S. E.; Baker, P. J.; Stuitje, A. R.; Slabas, A. R.; Hawkes, T. R.; Rice, D. W. A mechanism of drug action revealed by structural studies of enoyl reductase. *Science* **1996**, *274*, 2107–2110.
- Baldock, C.; de Boer, G.-J.; Rafferty, J. B.; Stuitje, A. R.; Rice, D. W. Mechanism of action of diazaborines. *Biochem. Pharm.* **1998**, *55*, 1541–1549.
- McMurry, L. M.; Oethinger, M.; Levy, S. B. Triclosan targets lipid synthesis. *Nature* **1998**, *394*, 531–532.
- Heath, R. J.; Yu, Y.-T.; Shapiro, M. A.; Olson, E.; Rock, C. O. Broad spectrum antimicrobial biocides target the FabI component of fatty acid synthesis. *J. Biol. Chem.* **1998**, *273*, 30316–30320.
- Levy, C. W.; Roujeinikova, A.; Sedelnikova, S.; Baker, P. J.; Stuitje, A. R.; Slabas, A. R.; Rice, D. W.; Rafferty, J. B. Molecular basis of triclosan activity. *Nature* **1999**, *398*, 383–384.
- McMurry, L. M.; McDermott, P. F.; Levy, S. B. Genetic evidence that InhA of *Mycobacterium smegmatis* is a target for FabI. *Antimicrob. Agents Chemother.* **1999**, *43*, 711–713.
- Slater-Radosti, C.; Van Aller, G.; Greenwood, R.; Nicholas, R.; Keller, P. M.; DeWolf, W. E., Jr.; Fan, F.; Payne, D. J.; Jaworski, D. D. Biochemical and genetic characterisation of the action of triclosan on *Staphylococcus aureus*. *J. Antimicrob. Chemother.* **2001**, *48*, 1–6.
- Heath, R. J.; Su, N.; Murphy, C. K.; Rock, C. O. The enoyl-[acyl-carrier-protein] reductases FabI and FabL from *Bacillus subtilis*. *J. Biol. Chem.* **2000**, *275*, 40128–40133.
- Bhat, G. P.; Surolia, N. Triclosan and fatty acid biosynthesis in *Plasmodium falciparum*: new weapon for an old enemy. *J. Biosci.* **2001**, *26*, 1–3.
- McLeod, R.; Muench, S. P.; Rafferty, J. B.; Kyle, D. E.; Mui, E. J.; Kirisits, M. J.; Mack, D. G.; Roberts, C. W.; Samuel, B. U.; Lyons, R. E.; Dorris, M.; Milhous, W. K.; Rice, D. W. Triclosan inhibits the growth of *Plasmodium falciparum* and *Toxoplasma gondii* by inhibition of Apicomplexan FabI. *Int. J. Parasitol.* **2001**, *31*, 109–113.
- Surolia, N.; Surolia, A. Triclosan offers protection against blood stages of malaria by inhibiting enoyl-ACP reductase of *Plasmodium falciparum*. *Nat. Med.* **2001**, *7*, 167–173. (For corrections to this paper, see *Nat. Med.* **2001**, *7*, 636).
- Suguna, K.; Surolia, A.; Surolia, N. Structural basis for triclosan and NAD binding to enoyl-ACP reductase of *Plasmodium falciparum*. *Biochem. Biophys. Res. Commun.* **2001**, *283*, 224–228.
- Heerding, D. A.; Chan, G.; DeWolf, W. E., Jr.; Fosberry, A. P.; Janson, C. A.; Jaworski, D. D.; McManus, E.; Miller, W. H.; Moore, T. D.; Payne, D. J.; Qiu, X.; Rittenhouse, S. F.; Slater-Radosti, C.; Smith, W.; Takata, D. T.; Vaidya, K. S.; Yuan, C. C. K.; Huffman, W. F. 1,4-Disubstituted imidazoles are potential antibacterial agents functioning as inhibitors of enoyl acyl carrier protein reductase (FabI). *Bioorg. Med. Chem. Lett.* **2001**, *11*, 2061–2065.
- Seefeld, M. A.; Miller, W. H.; Newlander, K. A.; Burgess, W. J.; Payne, D. J.; Rittenhouse, S. F.; Moore, T. D.; DeWolf, W. E., Jr.; Keller, P. M.; Qiu, X.; Janson, C. A.; Vaidya, K.; Fosberry, A. P.; Smyth, M. G.; Jaworski, D. D.; Slater-Radosti, C.; Huffman, W. F. Inhibitors of bacterial enoyl acyl carrier protein reductase (FabI): 2,9-disubstituted 1,2,3,4-tetrahydropyrido[3,4-b]indoles as potential antibacterial agents. *Bioorg. Med. Chem. Lett.* **2001**, *11*, 2241–2244.
- Miller, W. H.; Ku, T. W.; Ali, F. E.; Bondinell, W. E.; Calvo, R. R.; Davis, L. D.; Erhard, K. F.; Hall, L. B.; Huffman, W. F.; Keenan, R. M.; Kwon, C.; Newlander, K. A.; Ross, S. T.; Samanen, J. M.; Takata, D. T.; Yuan, C.-K. Enantiospecific synthesis of SB 214857, a potent, orally active, nonpeptide fibrinogen receptor antagonist. *Tetrahedron Lett.* **1995**, *36*, 9433–9436.
- Samanen, J. M.; Ali, F. E.; Barton, L. S.; Bondinell, W. E.; Burgess, J. L.; Callahan, J. F.; Calvo, R. R.; Chen, W.; Chen, L.; Erhard, K.; Feuerstein, G.; Heys, R.; Hwang, S.-M.; Jakas, D. R.; Keenan, R. M.; Koster, P. F.; Ku, T. W.; Kwon, C.; Lee, C.-P.; Miller, W. H.; Newlander, K. A.; Nichols, A.; Parker, M.; Peishoff, C. E.; Rhodes, G.; Ross, S.; Shu, A.; Simpson, R.; Takata, D.; Vasko-Moser, J. A.; Valocik, R. E.; Yellin, T. O.; Uzinskas, I.; Venslavsky, J. W.; Wong, A.; Yuan, C.-K.; Huffman, W. F. Potent, selective, orally active 3-oxo-1,4-benzodiazepine GPIIb/IIIa integrin antagonists. *J. Med. Chem.* **1996**, *39*, 4867–4870.
- Brewster, J. H.; Ciotti, C. J., Jr. Dehydrations with aromatic sulfonyl halides in pyridine. A convenient method for the preparation of esters. *J. Am. Chem. Soc.* **1955**, *77*, 6214–6215.
- Ku, T. W.; Miller, W. H.; Bondinell, W. E.; Erhard, K. F.; Keenan, R. M.; Nichols, A. J.; Peishoff, C. E.; Samanen, J. M.; Wong, A. S.; Huffman, W. F. Potent non-peptide fibrinogen receptor antagonists which present an alternative pharmacophore. *J. Med. Chem.* **1995**, *38*, 9–12.
- Heck, R. F. Palladium-catalyzed vinylation of organic halides. *Org. React.* **1982**, *27*, 345–390.
- The *E. coli* FabI assay uses crotonoyl-CoA, rather than the natural substrate crotonoyl-ACP, as the substrate. See the Experimental Section for details.
- Roujeinikova, A.; Levy, C. W.; Rowsell, S.; Sedelnikova, S.; Baker, P. J.; Minshull, C. A.; Mistry, A.; Colls, J. G.; Camble, R.; Stuitje, A. R.; Slabas, A. R.; Rafferty, J. B.; Pauptit, R. A.; Viner, R.; Rice, D. W. Crystallographic analysis of triclosan bound to enoyl reductase. *J. Mol. Biol.* **1999**, *294*, 527–535.

- (31) Qiu, X.; Janson, C. A.; Court, R. I.; Smyth, M. G.; Payne, D. J.; Abdel-Meguid, S. S. Molecular basis for triclosan activity involves a flipping loop in the active site. *Protein Sci.* **1999**, *8*, 2529–2532.
- (32) Heath, R. J.; Rubin, J. R.; Holland, D. R.; Zhang, E.; Snow, M. E.; Rock, C. O. Mechanism of triclosan inhibition of bacterial fatty acid synthesis. *J. Biol. Chem.* **1999**, *274*, 11110–11114.
- (33) Ward, W. H. J.; Holdgate, G. A.; Rowsell, S.; McLean, E. G.; Pauptit, R. A.; Clayton, E.; Nichols, W. W.; Colls, J. G.; Minshull, C. A.; Jude, D. A.; Mistry, A.; Timms, D.; Camble, R.; Hales, N. J.; Britton, C. J.; Taylor, I. W. F. Kinetic and structural characteristics of the inhibition of enoyl (acyl carrier protein) reductase by triclosan. *Biochemistry* **1999**, *38*, 12514–12525.
- (34) Marcinkeviciene, J.; Jiang, W.; Kopcho, L. M.; Locke, G.; Luo, Y.; Copeland, R. A. Enoyl-ACP reductase (FabI) of *Haemophilus influenzae*: steady-state kinetic mechanism and inhibition by triclosan and hexachlorophene. *Arch. Biochem. Biophys.* **2001**, *390*, 101–108.
- (35) Studies in the steroid 5 α -reductase area have shown that amides can function as transition-state enolate mimetics. See the following: Rasmusson, G. H.; Reynolds, G. F.; Utne, T.; Jobson, R. B.; Primka, R. L.; Berman, C.; Brooks, J. R. Azasteroids as inhibitors of rat prostatic 5 α -reductase. *J. Med. Chem.* **1984**, *27*, 1701–1701.
- (36) The apparent K_i value was calculated from the estimated IC₅₀ value assuming competitive inhibition with the substrate crotonoyl-ACP. However, since detailed mechanistic studies could not be done, because of the low K_m of the substrate and limitations in the sensitivity of the assay, the true K_i value could not be determined.
- (37) Payne, D. J.; Miller, W. H.; Berry, V.; Brosky, J.; Burgess, W. J.; Chen, E.; DeWolf, W. E., Jr.; Fosberry, A. P.; Greenwood, R.; Head, M. S.; Heerding, D. A.; Janson, C. A.; Jaworski, D. D.; Keller, P. M.; Manley, P. J.; Moore, T. D.; Newlander, K. A.; Pearson, S.; Polizzi, B. J.; Qiu, X.; Rittenhouse, S. F.; Slater-Radosti, C.; Salyers, K. L.; Seefeld, M. A.; Smyth, M. G.; Takata, D. T.; Uzinskas, I. N.; Vaidya, K.; Wallis, N. G.; Winram, S. B.; Yuan, C. C. K.; Huffman, W. F. Discovery of a novel, potent class of antibacterial agents. *Antimicrob. Agents Chemother.* Submitted for publication.
- (38) DeWolf, W. E., Jr. Unpublished results.
- (39) Brunger, A. T. *X-PLOR*, a system for X-ray crystallography and NMR, version 3.1; Yale University Press: New Haven, CT, 1987.
- (40) Brunger, A. T.; Adams, P. D.; Clore, G. M.; DeLano, W. L.; Gros, P.; Grosse-Kunstleve, R. W.; Jiang, J. S.; Kuszewski, J.; Nilges, M.; Pannu, N. S.; Read, R. J.; Rice, L. M.; Simonson, T.; Warren, G. L. Crystallography & NMR system: A new software suite for macromolecular structure determination. *Acta Crystallogr.* **1998**, *D54*, 905–921.

JM020050+